The Ocular Surface
A JOURNAL OF REVIEW, LIVING LABORATORY SCIENCE, CLINICAL SCIENCE, AND CLINICAL PRACTICE

Development of an *in vitro* model to study the biological effects of blinking

Guoting Qin, Hasna Baidouri, Adrian Glasser, VijayKrishna Raghunathan, Carol Morris, Inna Maltseva, Alison M. McDermott

PII: S1542-0124(17)30117-9

DOI: 10.1016/j.jtos.2017.12.002

Reference: JTOS 276

To appear in: *Ocular Surface*

Received Date: 2 May 2017

Revised Date: 12 October 2017

Accepted Date: 31 December 2017

Please cite this article as: Qin G, Baidouri H, Glasser A, Raghunathan V, Morris C, Maltseva I, McDermott AM, Development of an *in vitro* model to study the biological effects of blinking, *Ocular Surface* (2018), doi: 10.1016/j.jtos.2017.12.002.

Original Research

Development of an *in vitro* model to study the biological effects of blinking

Guoting Qin[1], Hasna Baidouri[1], Adrian Glasser[1], VijayKrishna Raghunathan[1], Carol Morris[2], Inna Maltseva[2], Alison M. McDermott[1]

Footnotes:

1. The Ocular Surface Institute, University of Houston, College of Optometry, Houston, TX, 77204

2. CooperVision Inc, Pleasanton, CA

This study was supported by CooperVision, Scottsville, NY and National Institute of Health [CORE Grant EY007551].

Financial interests: The authors have no proprietary or commercial interests in any concept or product discussed in this article

Corresponding Author

Alison M. McDermott, Ph.D.
Golden-Golden Professor
Professor of Optometry and Vision Sciences
Professor of Biology and Biochemistry
The Ocular Surface Institute (TOSI)
University of Houston
College of Optometry
4901 Calhoun Road
Houston, TX 77204-2020
Telephone: +1 713 743 1974
Fax: +1 713 743 2053
Email: alison.mcdermott@northumbria.ac.uk

Present Addresses

Dr. Alison M. McDermott. Ellison Building EBA515, Faculty of Health & Life Sciences, Northumbria University, Newcastle-upon-Tyne, NE1 8ST, UK.

ABSTRACT.

Purpose: To develop a mechanical model in which a contact lens is swept over ocular surface cells under conditions that mimic the force and speed of the blink, and to investigate the resulting biological changes.

Methods: A computer controlled mechanical instrument was developed to hold a dish containing 3D cultured stratified human ocular surface epithelial cells, across which an arm bearing a contact lens was swept back and forth repeatedly at a speed and force mimicking the human blink. Cells were subjected to repeated sweep cycles for up to 1 h at a speed of 120 mm/s with or without an applied force of 19.6 mN (to mimic pressure exerted by upper eyelid), after which the cell layer thickness was measured, the cell layer integrity was investigated using fluorescent quantum dots (6 and 13 nm) and the phosphorylation levels of various protein kinases were analyzed by human phospho-kinase arrays. Data for selected kinases were further quantitated by enzyme immunoassays.

Results: The thickness of the cell layers did not change after exposure to sweep cycles with or without applied force. Quantum dots (6 and 13 nm) were able to penetrate the layers of cells exposed to sweep cycles but not layers of untreated control cells. The phosphorylation levels of HSP27 and JNK1/2/3 increased for cells exposed to sweep cycles with applied force compared to untreated control cells.

Conclusions: The *in vitro* mechanical instrument is a useful tool to investigate the effects of blinking on the ocular surface.

KEYWORDS. Biomechanical model, Corneal epithelial cells, Mechanical force, Protein kinase phosphorylation,

1. INTRODUCTION

Blinking is essential for maintaining the health and well-being of the eye.[1-4] Each blink spreads tears over the entire ocular surface to create a smooth optical surface, helping to keep the eyes moist and lubricated.[3, 4] Blinking also clears away any debris and irritants.[3, 4] The speed and frequency of the blink vary quite considerably among human subjects and with methodology and specific experimental parameters. Reasonable averages are a spontaneous blink rate of 14-15 blinks/minute and a blink speed (taking into account both up and down phases) of 120 mm/second.[5, 6] Various studies have reported different measures of forces exerted on the ocular surface by the eye lids. One study reported a pressure of 50 mmHg (equivalent to 6.67 mN/mm^2 or 0.68 gf/mm^2) or more during a hard lid squeeze,[7] while another reported between 2 and 80 grams of loading force (i.e., between 19.6 mN and 784.5 mN loading force) ranging from a normal blink to a hard blink.[8] It is important to note that a number of forces are present at the ocular surface during blinking that depend on a variety of factors, such as ocular surface roughness, tear film thickness, composition and viscosity, lid wiper geometry, blink rate, surface mucins on ocular surface cells, and presence or absence of a contact lens. These factors act in tandem to regulate the exertion and distribution of the applied forces and dictate the health of the ocular surface. A detailed review of the contribution of individual factors can be found in Pult et al.[9]

A variety of factors can influence blinking, including everyday activities such as reading,[10] ocular surface disease such as dry eye,[11] and contact lens wear.[12] As the eyelid moves across the ocular surface during a blink, it creates a mechanical force on the contact lens, which moves and deforms the lens in a way crucial for post-lens tear film exchange, thus improving comfort during contact lens wear.[9] Moreover, the force generated on the contact lens during blinking is also transferred onto the ocular surface cells, and has both a normal and tangential component.[13] Furthermore, the movement and deformation of the contact lens during blinking induce tear fluid motion that creates shear pressure on the ocular surface cells.[14] Corneal epithelial cells under varying degrees of shear stress showed altered cytoskeleton and migratory behavior,[15] delayed wound healing,[16] and gross damage.[17]

Overall, it is well established that cells respond to the biophysical and biochemical properties of their microenvironment,[18] but little is known about how ocular surface cells respond to the mechanical stress of a blink, and the added stress in the presence of a contact lens at the molecular level. Therefore the purpose of this study was to develop a stratified human corneal

epithelial cell (HCEC) culture based model that utilizes dynamic conditions mimicking the force and speed of the blink so that the mechanical effects of blinking can be determined at the cellular level.

2. MATERIAL AND METHODS

2.1. Development of the *in vitro* Mechanical Model

A high-speed linear actuator and accompanying controller (Physik Instruments GmbH & Co. KG, Germany, Figure 1) were employed as the driver for the movement of an arm bearing a contact lens over the ocular cells *in vitro*, which was controlled by a customized Matlab program (Mathworks, R2014b, Figure 2). An apparatus was designed around the actuator, which allowed for precise control of the magnitude of the force applied that was read by a laboratory scale (Figure 1) and recorded by the Matlab program. The elastic moduli of the human cornea and eyelid[19, 20] were represented by a polyacrylamide gel with an elastic modulus of 25.50 ± 1.81 kPa placed underneath the cells, and a 1% agarose gel (elastic modulus 24.06 ± 5.4 kPa) placed between the contact lens and the arm tip. The fabrication of polyacrylamide gels was performed using formulations described previously.[21] Prior to use, the elastic moduli of polyacrylamide and agarose gels were validated using Atomic Force Microscopy [MFP-3D Bio (Asylum Research), BioScope Resolve (Bruker Nano), Santa Barbara, CA] as described previously.[21, 22] Finally, the entire apparatus was housed inside an incubator set at 37°C with humidity maintained using a water pan inside the incubator. The incubator also housed a CCTV camera for convenient monitoring of the movement of the actuator when the incubator door was closed during an experiment (Figure 2).

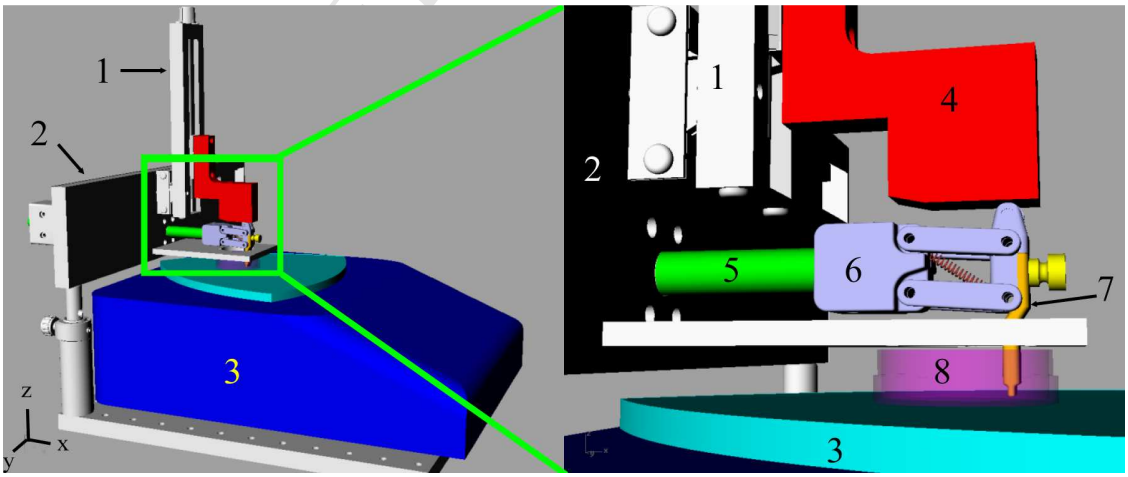

Figure 1. Illustration of the *in vitro* model system developed to study the effects of blinking on HCEC. Aluminum housing units **1** and **2** were used to stabilize the linear actuator **5** and arm guide **4**. **1** slides along **2** to allow positioning of the culture insert. **4** is fastened to **1** and its vertical location is controlled by the screw on top of **1**, which defines the magnitude of the force applied. The shaft on the actuator **5** pushes arm holder **6** along the arm guide **4**. A contact lens is stabilized on the tip of arm **7** that moves with **6**. The contact lens can be set to be either in contact with (applying force) or not in contact with cells (no force) in the culture insert **8**. Compliant gels (not shown in the figure) were placed underneath the cells (polyacrylamide gel with an elastic modulus of 25 kPa) and between the contact lens and arm tip (agarose gel) to represent the mechanical properties of the human cornea and eyelid.

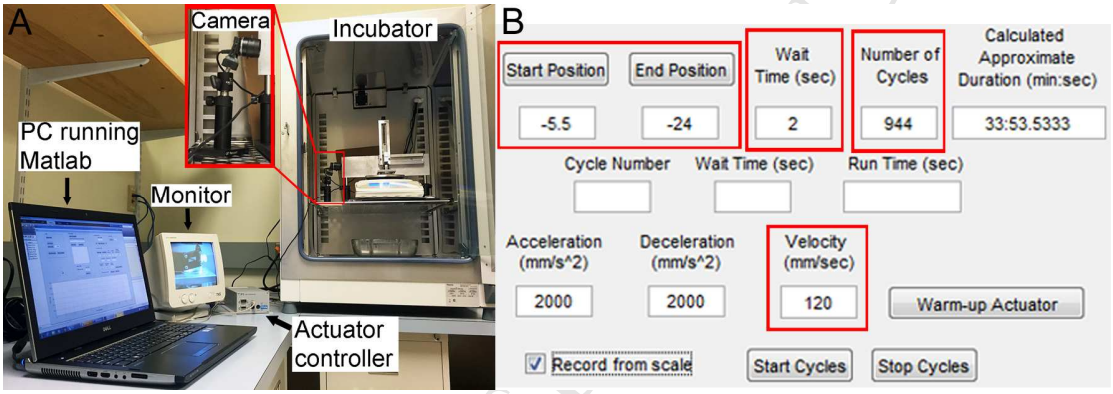

Figure 2. The *in vitro* biomechanical force model system. (A) The experimental setup, and B) the graphical user interface (GUI) of the Matlab program to control the movement of the linear actuator. The PC controlled the actuator and recorded the force applied to the cells. A CCTV camera in the incubator allowed for the movement of the actuator to be visualized on an external monitor when the incubator door was closed. The travel distance (defined by the starting and end positions), frequency (defined by the wait time between sweeps), duration (defined by the number of cycles) and velocity were set in the Matlab program GUI and are highlighted in red boxes.

2.2. Cell Culture and Use of Cells in the Mechanical Model

A validated telomerase immortalized human corneal epithelial cell line (hTCEpi) was used.[23] Briefly, cells were routinely maintained in KGM-2 culture media (Lonza Ltd., Switzerland) containing 0.15 mM Ca^{2+}. One million hTCEpi cells in 1.5 mL of culture medium were passed

into collagen-coated culture inserts (24-mm diameter, 3.0 μm pore size, Corning Inc. Corning, NY) that were submersed in 2 mL of culture medium in the wells of a 6-well plate. The membrane of the inserts is polytetrafluoroethylene (PTFE) that is pre-coated with collagen by the manufacturer (elastic modulus 11.30 ± 3.16 MPa). Cells were incubated at 37 °C with 5% CO_2 overnight, then the medium was changed to KGM-2 containing 1.15 mM Ca^{2+}. The medium was changed every other day for 7 days. To promote stratification, after 7 days the medium was removed from the upper chamber of the culture insert, exposing the cells to an air-liquid interface. The 1 mL of medium underneath the culture insert was changed every day during air-lifting for 7 days.

To perform an experiment, a culture insert with 1 mL culture medium covering the cells was mounted in the instrument and stabilized on a stainless steel holder, and positioned on the polyacrylamide gel in a petri-dish with ~ 5 mL culture medium. The large volume (1 mL) was necessary to fully cover cells on the insert and have enough depth (~ 2 mm) to immerse the contact lens (Biomedics 55, CooperVision, Scottsville, NY) stabilized at the arm tip. During the experiment, the arm tip moved back and forth to its original position (a sweep cycle) at a defined speed of 120 mm/s.[5, 6, 24, 25] The travel distance and resting time between sweeps were 18.5 mm, and 2 s, respectively.[26] Please note that by adopting the above sweeping parameters, the theoretical number of sweep cycles per min is 26. However, due to the acceleration and deceleration processes of the actuator resulting in a slower average speed (less than 120 mm/s), the experimental number of sweep cycles per min was calculated to be 16. The design and size of the arm bearing the contact lens limited the contact area with the cells to a central strip (approximately 1 cm by 2 cm) of the insert. Therefore, at the end of the experiment, the central strip of the insert membrane over which the contact lens moved during the experiment was cut out and the cells were harvested for further analysis. For cells subjected to the sweeping motion without applied force (i.e., 0 gram-force [equivalent to 0 mN] and labeled as “0 mN” hereafter), the arm bearing the contact lens was positioned above the cells immersed in the culture media; hence, these cells were not subjected to any contact or force from the contact lens but were subjected to shear stress caused by turbulence of the culture media. To exert force on the cells, the arm bearing the lens was carefully moved into position until the contact lens touched the cells with the required amount of normal force (typically 2 gram-force (equivalent to 19.6 mN) and labeled as “19.6 mN” hereafter). The force was measured by the scale underneath and shown on

the scale screen. Furthermore, the force was continuously read during sweeping and recorded by the Matlab program. Stratified cells on culture inserts, which were not subjected to any manipulation, served as controls.

Preliminary studies were conducted, subjecting cells to 300, 500, 600 and 944 sweep cycles with or without the force of 19.6 mN, after which cells were harvested and analyzed using phosphokinase arrays. Changes in phosphorylation were detectable at 300 sweep cycles and the change relative to control was greater with higher numbers of sweep cycles (data not shown), therefore subsequent experiments were conducted with 944 sweep cycles unless otherwise stated.

2.3. Cell Layer Thickness Measurement

Samples that were subjected to sweep cycles with or without force, as well as control samples, were fixed in 2 mL 0.1 mM sodium cacodylate with 2.5% glutaraldehyde and 20 mM calcium chloride for 30 min at room temperature followed by washing three times with 2 mL 0.1 mM sodium cacodylate buffer. A strip of ~3 mm × 1.5 cm was cut out from each insert membrane and placed in a 1.5 mL tube individually. All samples were incubated in 1 mL cacodylate buffer containing 0.75% potassium ferrocyanide, 0.15 M sodium cacodylate, 2 mM calcium chloride and 1% osmium tetroxide for 1 h on ice. After washing with 1 mL Milli-Q water at room temperature three times, the samples were incubated in 1 mL thiocarbohydrazide solution for 10 min at room temperature followed by washing with 1 mL Milli-Q water three times. The samples were then incubated with 1 mL 1% osmium tetroxide for 15 min at room temperature followed by washing with water three times. Then the samples were placed in 1 mL 1% uranyl acetate and stored at 4 °C overnight. The next day, the samples were washed with Milli-Q water three times and incubated in a lead aspartate staining solution at 60 °C for 30 min followed by washing with Milli-Q water three times. All samples were dehydrated using ice-cold solutions of freshly prepared 20%, 50%, 70%, 90% and 100% acetone for 5 min each, and then placed in 100% acetone at room temperature for another 10 min. All samples were placed sequentially in 25%, 50%, and 75% resin in acetone overnight, then placed in 100% resin for two days with daily changes. All samples were embedded in resin in a silicone rubber mold at 60 °C for 48 h. The blocks were cut into 200 nm sections and stained with Toluidine blue, and observed using a DeltaVision Spectris Core inverted microscope (Applied Precision, Issaquah, WA). The cell layer thickness was measured using softWoRx 1.0 software. For each sample, at least five

images were taken at various locations from at least two sections, and three measurements were taken for each image. The data were expressed as the mean thickness of more than 15 measurements.

2.4. Quantum Dot (QD) Imaging

Quantum dots were used to determine whether exposure to sweep cycles with and without force affected cell layer integrity. Stratified hTCEpi cells on culture inserts were incubated with QDs (0.08 μM) with a diameter of 3.5 nm (fluoresce green, Sigma-Aldrich, Co. St. Louis, MO.), 6 nm (fluoresce red, Sigma-Aldrich, Co.) and/or 13 nm (fluoresce green, Life Technologies, Inc. Carlsbad, CA) in 1 mL KGM-2 culture medium containing 1.15 mM Ca^{2+} at 37 °C with 5% CO_2 for 1 h. Based on the information provided by the vendors, QDs of 13 nm are nearly spherical, and QDs of 3.5 and 6 nm are irregularly shaped. Cells were washed with 2 mL PBS three times to remove any excess QDs. The membrane was cut out of each insert and embedded in Tissue-Tek Optimal Cutting Temperature (OCT) compound (Sakura Finetck USA Inc. Torrance, CA). The OCT blocks were then cut into 10 μm sections on a cryostat, placed on slides, covered with Vectashield mounting medium for fluorescence containing a nuclear fluorescent dye DAPI (Vector Laboratories Inc. Burlingame, CA), and sealed with cover slips. All sections were imaged using a fluorescence microscope (Olympus IX71, Japan). This microscope cannot resolve individual QDs because of their small size thus the fluorescence signals were from clusters of QDs that were formed when they traveled through the cell layers.

Some samples were also stained with rhodamine labeled actin stain phalloidin (Life Technologies, Inc. Carlsbad, CA). After exposure to sweep cycles, the cells were incubated with QDs as described above followed by the phalloidin solution for 20 min. Cells were washed with 2 mL PBS three times, embedded in OCT and imaged following the procedure described above.

2.5. Protein Array and Enzyme-linked Immunosorbent Assay (ELISA)

Immediately after exposure to sweep cycles with or without force as described above, the area of the insert membrane that was in contact with the arm bearing the contact lens was cut out from each sample, and placed into 1.5 mL Eppendorf tubes. Cells without any manipulation served as controls. Entire membranes from control samples were cut out and placed in 1.5 mL Eppendorf tubes. All samples were frozen in liquid nitrogen and stored at -80 °C until analysis. On the day

of testing using a Human Phospho-Kinase Array kit (R&D systems, Minneapolis, MN.), samples were lysed using the lysis buffer supplied in the kit. Cell lysate from 2-4 inserts that were subjected to the same treatment was pooled to obtain sufficient protein for analysis. The total amount of protein in each sample was determined using the BCA assay. The same amount of protein for control and test samples was loaded on the arrays. The assays were performed as per the manufacturer's instructions and the membranes exposed to x-ray film for detection of the chemiluminescent signal. A sample x-ray film is shown in Figure S1 (Supporting Information). To determine the phosphorylation of the proteins on the array, a custom Matlab program was used to analyze scanned images of the developed x-ray film. Briefly, each target protein kinase presented itself as two duplicate spots, and the darkness of the spots indicated its relative phosphorylation level in the sample. The Matlab program located each target spot on the images based on the parameters of the array template provided by the manufacturer (Supporting Information, Table S1), and calculated the signal intensity of each spot individually. Then the signal intensities from two duplicate spots were corrected by subtracting background signal and averaged, and exported as the mean signal intensity for each target protein kinase on the film.

The data for selected protein kinases (HSP27, JNK1/2/3, p38α, and cyclic adenosine monophosphate response element-binding protein (CREB)) were then confirmed by quantitating the phosphorylation level by ELISA (R&D Systems, Minneapolis, MN). All samples that were subjected to sweep cycles with or without force, as well as control samples, were processed and stored as described above. On the day of testing, samples were lysed using the buffer supplied in each kit for each target protein kinase. Relevant samples were also pooled to obtain sufficient amount of protein for analysis. The total amount of protein in each sample was determined using the BCA assay. The same amount of protein for control and test samples was used for each assay. The assay was performed and the phosphorylation level of each protein kinase was calculated per the manufacturer's instructions.

2.6. Statistical analysis

The data are expressed as mean ± SD. Differences in the phosphorylation levels of HSP27, CREB, JNK1/2/3, and p38α as well as cell layer thicknesses between control and treated samples were evaluated by one-way ANOVA followed by Tukey's test where significance was found with $p < 0.05$.

3. RESULTS

3.1. Cell Layer Thickness

A montage of images of toluidine blue stained sections showing the 3D cultured hTCEpi cells on the insert membrane is presented in Figure 3A. The thickness of the cell layer was not uniform across the insert membrane with the number of layers ranging from 2 to 7. The average cell layer thicknesses were 16.3 ± 3.6, 25 ± 1.0, and 24 ± 7.8 μm for the control and cells exposed to 944 sweep cycles with forces of 0 mN and 19.6 mN respectively (Figure 3B). No statistically significant thickness differences were observed between control and treated samples indicating that exposure to a force of 19.6 mN did not induce gross damage to the stratified layers.

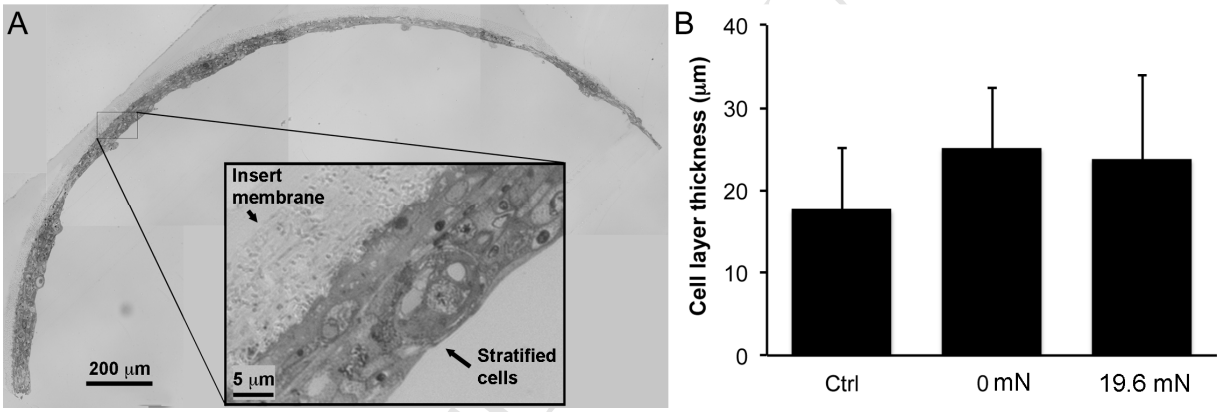

Figure 3. Bright field image of 3D cultured hTCEpi cells on a culture insert and cell layer thickness measurements. A) A montage of toluidine blue stained section images showing the control cells on a membrane. The membrane became curved when embedded in resin during the sample preparation process described in Methods. The inset shows a higher magnification image of one area on the membrane. B) Cell layer thicknesses of samples without treatment (Ctrl) and exposed to sweep cycles with force of 0 mN or 19.6 mN. Data are expressed as mean ± SD from three independent experiments. Statistical analysis was performed using one-way ANOVA but no significant differences were observed (p=.14).

3.2. Quantum Dot Imaging

The use of QDs was previously demonstrated to be a valid method to evaluate cultured epithelial cell sheet barrier function.[27] In a preliminary study, hTCEpi cells were incubated with QDs of 3.5, 6, or 13 nm diameter; QDs with a diameter of 3.5 nm penetrated through the cell

layers (data not shown), while QDs with a diameter of 6 or 13 nm did not. Therefore, QDs of 3.5 nm were too small to evaluate cell layer integrity. As shown in Figure 4A, the red and green fluorescence of the 6 and 13 nm QDs, respectively, remained above the blue fluorescence of the DAPI stained cell nuclei indicating that these QDs stayed on top and did not penetrate the intact junctions of the cell layers. Cells on insert membranes were incubated with 2.5 mM EDTA for 3 h to disrupt cellular junctions followed by incubation with 6 or 13 nm QDs. We observed that QDs of both sizes were then able to penetrate through the cell layers, indicating disruption of the layers (Figure 4B). The 6 and 13nm QDs were then used to investigate layer integrity of cells subject to sweep cycles. For samples subjected to 944 sweep cycles without (0 mN, Figures 4C&4D) or with (19.6 mN, Figures 4E&4F) force, there were always two patterns of fluorescent signal observed in the area where the arm bearing the contact lens was in contact with the cells. There were locations where the green and red fluorescence of the QDs was above the blue fluorescence from the cell nuclei indicating that in these areas the QDs did not penetrate through the cell layers as shown in the examples in Figure 4 C&4E. Also, there were locations where the green and red fluorescence from the QDs overlapped with the blue fluorescence from the cell nuclei indicating that in these particular regions the QDs penetrated through cell layers as shown in the examples in Figure 4D & F.

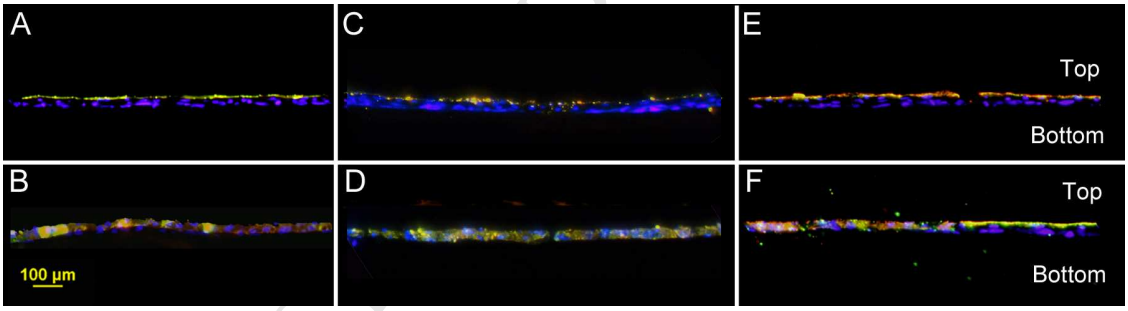

Figure 4. QD imaging of 3D cultured hTCEpi cells. Fluorescence images of (A) control, (B) cells treated with EDTA, (C) and (D) different areas of cells on the membrane in contact with the contact lens during 944 sweep cycles without force, (E) and (F) different areas of cells on the membrane in contact with the contact lens during 944 sweep cycles with force of 19.6 mN. Blue: DAPI nuclear stain, Red: 6 nm QDs, Green: 13 nm QDs. Top and Bottom in the figure indicate the top and bottom of the cell layers. These are representative data from three independent experiments

We also investigated the cell layer integrity of stratified corneal epithelial cells in areas that were not in contact with the arm bearing the contact lens during sweep cycles without (0 mN) and with (19.6 mN) force. In this study, rhodamine labeled actin stain phalloidin was used for better visualization of the locations of the QDs (only 13 nm QDs were tested). As shown in Figure 5, two patterns of fluorescent signal were also found. There were locations where the green fluorescence of the QDs remained above the blue fluorescence from the cell nuclei and red fluorescence from actin staining indicating that the QDs did not penetrate through the cell layers in those areas, as shown in Figure 5 A &B. Also, there were locations where the green fluorescence from QDs overlapped with the blue fluorescence from the cell nuclei and red actin staining indicating that QDs penetrated through cell layers, as shown in Figure 5C & D.

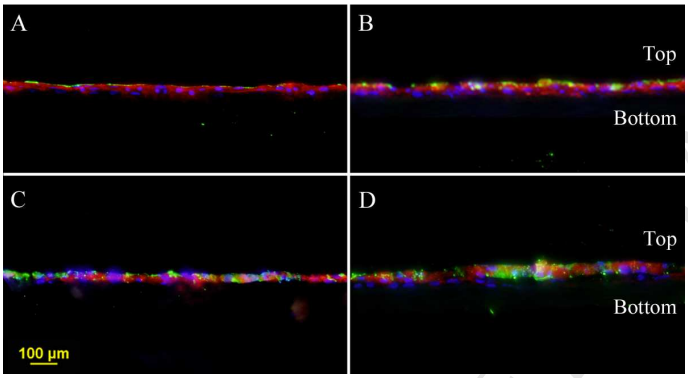

Figure 5. QD imaging of 3D cultured hTCEpi cells in areas that were not in contact with the contact lens during exposure to sweep cycles. Fluorescence images of areas that were not in contact with the contact lens during 944 sweep cycles without force (A and C) and with force of 19.6 mN (B and D). Blue: DAPI nuclear stain, Red: rhodamine labeled phalloidin staining, Green: 13 nm QDs. Top and Bottom in the figure indicate the top and bottom of the cell layers. These are representative data from two independent experiments.

3.3. Protein array and ELISA

Human Phospho-Kinase Array kits were used to detect the relative levels of phosphorylation of 43 different kinases and two related proteins. As modification of signaling proteins occurs prior to changes in effector protein levels, due to the short sweep duration (1 h), we chose to determine alterations in phospho-kinase levels. Among the 45 targets, several of the kinases,

such as HSP27, JNK1/2/3, and p38α, showed consistent changes (in this case increased) among three independent experiments whereas for others, such as CREB, the changes were variable (Supporting information, Table S2). As the array only provides relative changes in phosphorylation levels, we used ELISAs to quantitate the changes in specific kinases. As shown in Figure 6, HSP27 and JNK1/2/3, but not CREB nor p38α, showed significantly increased phosphorylation in cells treated with force of 19.6 mN for 944 cycles compared to control samples. No statistically significant increase in phosphorylation for any of the four kinases was found in cells exposed to force of 0 mN compared to control samples, although the levels were greater than in controls. Phosphorylation of HSP27 and JNK1/2/3 was increased in cells exposed to sweep cycles with a force of 19.6 mN compared to cells exposed to sweep cycles without force but this only reached statistical significance for HSP27. For the cells that were not in contact with the contact lens during sweeping, there were no significant differences in the phosphorylation levels of HSP27 and JNK1/2/3 among control and cells subjected to 0 mN and 19.6 mN (data not shown).

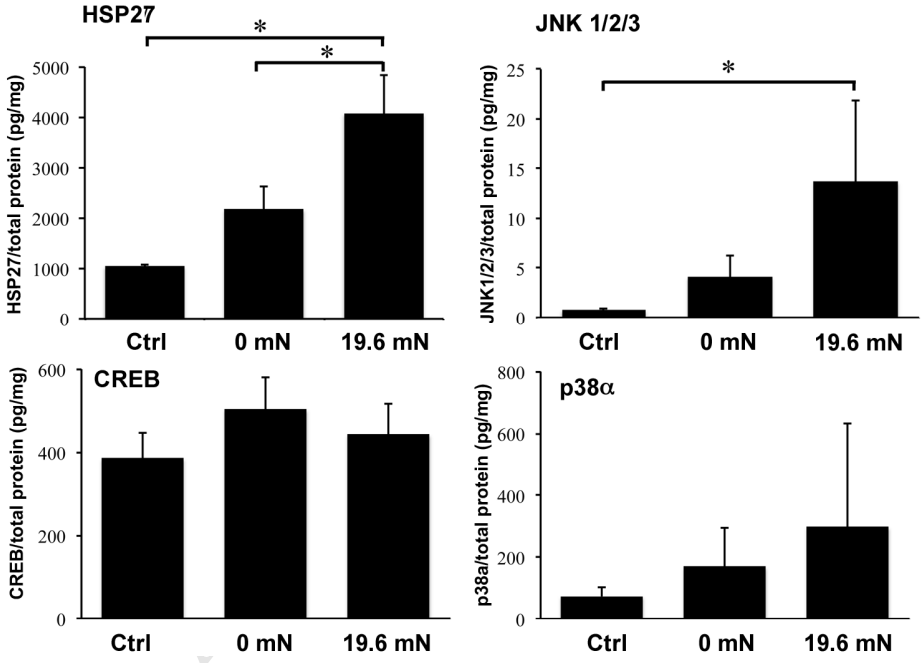

Figure 6. Quantification of phosphorylation levels of HSP27, JNK1/2/3, CREB, and p38α from control and hTCEpi cell samples exposed to 944 sweep cycles (0 mN and 19.6 mN). Data are expressed as mean ± SD from three independent experiments. Statistical analysis was

performed using one-way ANOVA followed by Tukey's test where significance was found. *p<.05.

4. DISCUSSION

Mechanical stress is exerted onto the cornea by the movement of the eyelids during blinking, and likely increases with contact lens wear.[9] In the present study, we developed an *in vitro* system to investigate the effects of mechanical stress on cellular characteristics. In this system, individual parameters (duration, speed, distance, frequency, and the applied force) of the arm bearing the contact lens were independently controlled. Literature values for the frequency and speed of the blink vary considerably based on the methodology and specific experimental parameters. It has also been reported that contact lens wearers have higher blink rates.[28, 29] In this study, we employed an "eye blink" rate in the region of 14-15 eye blinks/minute[26] and a preset blink speed of approximately 120 mm/s.[5, 6, 24, 25] Moreover, the reported normal pressure exerted during blinking varies widely (9.8 - 784.5 mN) in the literature.[7, 30] Herein, a relatively low force of 19.6 mN was used based on the data of Shaw et al.[30] In the case of sweep cycles without force, the movement of the arm bearing the contact lens created turbulence in the culture media inducing shear stress on the cells. The shear stress was estimated to be in the range of 0.57 – 1.10 dyne/cm^2 (See Supporting Information for detailed calculation), which is comparable to reported shear stress values on corneal epithelial cells.[15,31]

Cell layer thickness was measured after exposure to sweep cycles to ascertain if there was thinning of cell layers, which would indicate gross damage to the cells. Exposure with (19.6 mN) or without (0 mN) force for 50, 250, 500, and 944 sweep cycles did not result in cell layer thinning (data not shown for 50, 250 and 500 cycles). However, we noted the variation in the number of cell layers across the membranes, resulting in marked variations in the measured cell layer thicknesses. As this may mask the effect of force, especially as the force (19.6mN) applied in our experiments was at the lower end of the reported lid pressure values,[7, 30] we also tested the effect of larger forces (98.1 and 196.1 mN, equivalent to 10 and 20 gram-force respectively) to determine if changes could be visualized using our approach. We found that sweep cycles with larger forces did induce cell layer thinning, indicating severe damage (Supporting information, Figure S2). Therefore, we concluded that the low force applied in our experimental setup did not cause significant shear or subsequent damage to the cells.

While gross damage was not observed for cells subjected to force in our experimental setup, several modalities were employed to determine whether there were biological changes in the integrity of the cell layers as well as cellular structures. In preliminary studies, we investigated potential changes in the distribution of the cell junction protein ZO-1 and rearrangement of the actin cytoskeleton by immunostaining but did not observe any remarkable difference among cells with/without exposure to sweep cycles using this approach (data not shown). Recent studies reported cytoskeleton changes for monolayer cells grown on glass slides after 24 h exposure to shear stress.[15, 16] The results from those studies are not directly comparable to the present study due to different experimental parameters used. Our model utilized multiple layers of stratified cells and short time of exposure (1 h), and these may have contributed to the fact that we did not observe cytoskeleton changes.

We used QDs to probe cell layer integrity due to their unique advantages for imaging because of their defined sizes.[27] QDs with a diameter of 3.5 nm traveled freely through control cell layers, and therefore, were too small to provide any information on cellular integrity for cells subjected to sweep cycles. QDs with a diameter of 6 or 13 nm stayed on top of the layers of control cells, but penetrated through the layers if the cell junctions were disrupted by EDTA. Therefore, QDs of 6 and 13 nm were used to investigate cell layer integrity. Interestingly, we observed two patterns of fluorescence marking the location of the QDs in cells exposed to sweep cycles. In one, the fluorescent signal was within/below the cell layers, showing that the QDs penetrated through indicating compromised cell layer integrity. As we did not observe changes in ZO-1 staining, the penetration of QDs might be due to the change in the size of the paracellular space as shown by Duncan et al.[27] Whether this change is permanent or transient is not known and warrants further investigation. Alternatively, in other areas, the fluorescence from the QDs remained above the cells, indicating no penetration and existence of intact cell layers. One possible reason for this pattern is that the unevenness of the cell layers (Figure 3) may create weaker spots that are more readily prone to damage when subject to shear stress and mechanical forces. More significantly, we found that both patterns of fluorescence were present for cells exposed to sweep cycles with or without force of 19.6 mN. This indicates that cells responded not only to the force, but also to shear stress induced by the turbulence of the culture media. This observation was confirmed by imaging the cells on areas of the membrane that were not in contact with the contact lens during application of the downward normal force. Another reason

may be that the QDs were endocytosed and internalized by the corneal epithelial cells, although it is unlikely due to the short incubation time (1 h) and the negatively charged QD surfaces that are unfavorable for endocytosis. Passive uptake of charged/functionalized QDs by semi-confluent cell layers has been documented when used at very high concentrations over long time periods.[32-35] The likelihood of this in our system is minimal since the stratified corneal epithelial cells were exposed to a low concentration of non-modified QDs for a short period of time. Some localization of QDs within the cytosol in corneal epithelial cells may also be attributed to G-protein coupled receptor (GPCR) mediated endocytosis.[36] A growing body of literature documents the link between GPCRs, shear stress, and mechanotransduction through cytoskeletal remodeling,[37-40] leading us to infer that any internalization of QDs may be due to the applied force.

Thus, our data showed that although there was no gross damage (no reduction in cell layer thickness) after exposure to sweep cycles, shear stress as well as mechanical forces caused compromise of cell layer integrity. This phenomenon is unlikely to occur *in vivo* because: 1) corneal epithelial cells *in vivo* are more tightly coupled compared to the stratified cells *in vitro*; 2) *in vitro* experimental conditions are different from *in vivo* such as the solution volume (1 mL *in vitro* vs ~7 μl *in vivo*[41]) and solution composition (culture medium *in vitro* vs protein-containing tears *in vivo*), which may affect the magnitude of forces experienced by cells; 3) glycocalyx expressed by stratified cells *in vitro* may be different from glycocalyx *in vivo*, thus resulting in potential differences in barrier function.

Cellular changes at the molecular level were determined by measuring relative phosphorylation levels of various protein kinases by protein arrays and then confirming the changes in select kinases by ELISA. Significantly greater phosphorylation was observed for HSP27, JNK1/2/3, and p38, when the cells were subjected to a sweep-shear force. This response was further enhanced in the presence of the downward force of 19.6 mN. Phosphorylation of HSP27, p38, and JNK1/2/3 has been observed in a variety of cell types subjected to different stresses such as UV irradiation,[42-44] hyperosmotic stress,[45-48] oxidative stress,[49] injury,[50] and shear stress.[51] Transient up-regulation of phosphorylation of JNK has also been found upon corneal injury *in vivo*[52] and *in vitro*.[53] While we did not observe any changes in phosphorylation of CREB regardless of applied shear and downward forces, increased phosphorylation of CREB has been reported in chondrocytes,[54] osteoblasts,[55, 56] and vascular endothelial cells[36, 57, 58] under

mechanical and/or shear stress suggesting that not all stress responses are uniform across different cell types. Our data demonstrate that shear and mechanical forces are capable of triggering a stress response in corneal epithelial cells. Whether these alterations are cytoprotective or detrimental remains to be elucidated taking into consideration that differential blink forces (shear and downward) may be exerted on ocular surface cells under adverse conditions *in vivo*.

As a contact lens travels along the cornea with the eyelid during a blink, the tribological characteristics may transition between brush-to-brush lubrication and hydrodynamic lubrication,[9] which determines the friction experienced by cells. The transition between different lubrication mechanisms is determined by factors such as lens properties, blink velocity (slow vs. high), tear film composition and quality, and cell properties such as quality of mucins on the cell surface.[9, 59] Furthermore, the deposition of lipids and proteins from tear film to contact lenses also affects the hydration of the contact lens surface, thus the lubrication between the lens and cells. The intrinsic physicochemical properties of the lens material contribute towards the coefficient of friction and subsequent frictional force. Therefore, the surface and bulk properties of contact lenses affect the lubrication mechanisms during blinking, thus the forces experienced by cells. Consequently, cells may respond differently to different contact lens materials. In this study, we used one type of contact lens (Biomedics 55, Ocufilcon D) to test our in vitro biomechanical system. Biomedics 55 is a Group 4 hydrogel contact lens and was selected for the study because of its conventional characteristics in comparison to newer silicone hydrogels, which have very different mechanical and surface properties. It is likely that various materials (synthetic and biological) may indeed elicit different responses by cells of the ocular surface. That being said, this first study was performed to validate our model, establish baseline responses, and enhance our understanding of whether downward and shear forces have potent effects on cells. We anticipate using this model to systematically study the effect of each individual factor on cells in comprehensive future studies.

5. CONCLUSIONS

We developed an *in vitro* model to study the cellular effects of blinking on corneal epithelial cells. This model allows for independent control over the movement speed, frequency, duration and distance, which offers advantages to study the effect of each individual factor during

blinking. Using this model, we found that HCEC responded not only to shear stress created by fluid turbulence, but also to applied mechanical forces. No gross damage was observed under the experimental conditions employed; however, cells responded at the molecular level with altered levels of protein-kinase phosphorylation, suggesting that the blinking motion created stress and induced inflammation. It is feasible that such changes observed are an adaptive response when cells transition from a non-physiological static culture system to a more dynamic system that may be representative of physiological conditions in the native ocular surface. Further studies would be required to comprehensively understand the implications of such a response. This model is not limited to the study of ocular surface cells, but can be used to study the effects of mechanical forces on a wide variety of adherent cell types. Additionally, various materials can be tested by replacing the contact lens at the end of the arm tip. Therefore, this model provides us a useful tool to evaluate the cellular responses to mechanical forces under varying conditions and will be of benefit in elucidating their contribution to the pathology underlying ocular conditions such as contact lens discomfort and dry eye.

Supporting Information

The Human Phospho-Kinase Array assay results, shear stress estimation, and the cell layer thickness measurement for cells treated with forces up to 196.1 mN are included in the supporting information. This material is available free of charge via the Internet at http://pubs.acs.org.

ACKNOWLEDGMENT

We thank Mr. Chris Kuether for CAD design, machining and 3D printing, Dr. Alan Burns for access to the Delta Vision Spectris Core microscope and to Margaret Gondo and Evelyn Brown for assistance with sample preparation and microscopy. We are very grateful to Dr. Christopher Murphy of the University of California-Davis for advice and assistance on the preparation and validation of compliant gels by atomic force microscopy. We are grateful to Hope Queener for assistance with Matlab program [Core grant P30EY007551]. We thank Drs. Rodrigo Velez-Cordero and Bernardo Yañez-Soto of the Institute of Physics (University of San Luis Potosi) for measuring the viscosity of the culture medium.

REFERENCES

1. Ousler GW, Hagberg KW, Schindelar M, Welch D, Abelson MB. The Ocular Protection Index. Cornea. 2008;27:509-513.

2. Esteban A, Traba A, Prieto J. Eyelid movements in health and disease. The supranuclear impairment of the palpebral motility. Neurophysiol. Clin.-Clin. Neurophysiol. 2004;34:3-15.

3. Cher I. Fluids of the ocular surface: concepts, functions and physics. Clin. Exp. Ophthalmol. 2012;40:634-643.

4. Braun RJ. Dynamics of the tear film. In: Davis SH, Moin P (eds), Annual Review of Fluid Mechanics, Vol 44; 2012:267-297.

5. Kwon KA, Shipley RJ, Edirisinghe M, Ezra DG, Rose G, Best SM, et al. High-speed camera characterization of voluntary eye blinking kinematics. J. R. Soc. Interface 2013;10:6.

6. Nakamura Y, Matsuda J, Suzuki K, Toyoda H, Hakamata N, Shimamoto T, et al. Measurement of spontaneous blinks with a high-speed blink analyzing system. Nippon Ganka Gakkai zasshi 2008;112:1059-1067.

7. Miller D. Pressure of the lid on the eye. Arch Ophthalmol (Chicago IL: 1960) 1967;78:328-330.

8. Hung G, Hsu F, Stark L. Dynamics of the human eyeblink. Am J Optom Physiol Opt 1977;54:678-690.

9. Pult H, Tosatti SGP, Spencer ND, Asfour JM, Ebenhoch M, Murphy PJ, et al. Spontaneous blinking from a tribological viewpoint. Ocul Surf. 2015;13:236-249.

10. Argiles M, Cardona G, Perez-Cabre E, Rodriguez M. Blink rate and incomplete blinks in six different controlled hard-copy and electronic reading conditions. Invest Ophthalmol Vis Sci. 2015;56:6679-6685.

11. Rahman EZ, Lam PK, Chu CK, Moore Q, Pflugfelder SC. Corneal sensitivity in tear dysfunction and its correlation with clinical parameters and blink rate. Am J Ophthalmol. 2015;160:858-866.

12. Efron N, Jones L, Bron AJ, Knop E, Arita R, Barabino S, McDermott AM, Villani E, Willcox MD, Markoulli M; members of the TFOS International Workshop on Contact Lens Discomfort. The TFOS International Workshop on Contact Lens Discomfort: report of the contact lens interactions with the ocular surface and adnexa subcommittee. 2013;54:98-122.

13. Conway HD, Richman M. Effects of contact-lens deformation on tear film pressures induced during blinking. Am J Optom Physiol Opt. 1982;59:13-20.

14. Chauhan A, Radke CJ. Modeling the vertical motion of a soft contact lens. 2001;22:102-108.

15. Molladavoodi S, Robichaud M, Wulff D, Gorbet M. Corneal epithelial cells exposed to shear stress show altered cytoskeleton and migratory behaviour. PLoS One 2017;12:16.

16. Utsunomiya T, Ishibazawa A, Nagaoka T, Hanada K, Yokota H, Ishii N, et al. Transforming growth factor-beta signaling cascade induced by mechanical stimulation of fluid shear stress in cultured corneal epithelial cells. Invest Ophthalmol Vis Sci. 2016;57:6382-6388.

17. Cobb JA, Dunn AC, Kwon J, Sarntinoranont M, Sawyer WG, Tran-Son-Tay R. A novel method for low load friction testing on living cells. Biotechnol Lett. 2008;30:801-806.

18. Bukoreshtliev NV, Haase K, Pelling AE. Mechanical cues in cellular signalling and communication. Cell Tissue Res. 2013;352:77-94.

19. Last JA, Thomasy SM, Croasdale CR, Russell P, Murphy CJ. Compliance profile of the human cornea as measured by atomic force microscopy. Micron 2012;43:1293-1298.

20. Winkler M, Chai D, Kriling S, Nien CJ, Brown DJ, Jester B, et al. Nonlinear optical macroscopic assessment of 3-D corneal collagen organization and axial biomechanics. Invest Ophthalmol Vis Sci. 2011;52:8818-8827.

21. McKee CT, Wood JA, Shah NM, Fischer ME, Reilly CM, Murphy CJ, et al. The effect of biophysical attributes of the ocular trabecular meshwork associated with glaucoma on the cell response to therapeutic agents. Biomaterials 2011;32:2417-2423.

22. Chang YR, Raghunathan VK, Garland SP, Morgan JT, Russell P, Murphy CJ. Automated AFM force curve analysis for determining elastic modulus of biomaterials and biological samples. J. Mech. Behav. Biomed. Mater. 2014;37:209-218.

23. Robertson DM, Li L, Fisher S, Pearce VP, Shay JW, Wright WE, et al. Characterization of growth and differentiation in a telomerase-immortalized human corneal epithelial cell line. Invest Ophthalmol Vis Sci 2005;46:470-478.

24. Choi SH, Park KS, Sung MW, Kim KH. Dynamic and quantitative evaluation of eyelid motion using image analysis. Med Biol Eng Comput. 2003;41:146-150.

25. Guitton D, Simard R, Codere F. Upper eyelid movements measured with a search coil during blinks and vertical saccades. Invest Ophthalmol Vis Sci. 1991;32:3298-3305.

26. Doughty MJ. Spontaneous eyeblink activity under different conditions of gaze (eye position) and visual glare. Graefes Arch Clin Exp Ophthalmol. 2014;252:1147-1153.

27. Duncan TJ, Baba K, Oie Y, Nishida K. A novel method using quantum dots for testing the barrier function of cultured epithelial cell sheets. Invest Ophthalmol Vis Sci. 2015;56:2215-2223.

28. Hill RM. The quantitative blink. Int Contact Lens Clin. 1984;11:366-368.

29. Martin-Montanez V, Lopez-de La Rosa A, Lopez-Miguel A, Pinto-Fraga J, González-Méijome JM, González-García MJ. End-of-day dryness, corneal sensitivity and blink rate in contact lens wearers. Cont Lens Anterior Eye 2015;38:148-151.

30. Shaw AJ, Collins MJ, Davis BA, Carney LG. Eyelid pressure and contact with the ocular surface. Invest Ophthalmol Vis Sci. 2010;51:1911-1917.

31. Srinivas SP, Mutharasan R, Fleiszig S. Shear-induced ATP release by cultured rabbit corneal epithelial cells. In: Sullivan DA, Stern ME, Tsubota K, et al. (eds), Lacrimal Gland, Tear Film, and Dry Eye Syndromes 3: Basic Science and Clinical Relevance Part A and B. Boston, MA: Springer US; 2002:677-685.

32. Jaiswal JK, Mattoussi H, Mauro JM, Simon SM. Long-term multiple color imaging of live cells using quantum dot bioconjugates. Nat Biotechnol. 2003;21:47-51.

33. Nabiev I, Mitchell S, Davies A, Williams Y, Kelleher D, Moore R, et al. Nonfunctionalized nanocrystals can exploit a cell's active transport machinery delivering them to specific nuclear and cytoplasmic compartments. Nano Lett. 2007;7:3452-3461.

34. Delehanty JB, Medintz IL, Pons T, Brunel FM, Dawson PE, Mattoussi H. Self-assembled quantum dot-peptide bioconjugates for selective intracellular delivery. Bioconjugate Chem. 2006;17:920-927.

35. Helmick L, Antúnez de Mayolo A, Zhang Y, Cheng CM, Watkins SC, Wu C, et al. Spatiotemporal response of living cell structures in Dictyostelium discoideum with semiconductor quantum dots. Nano Lett. 2008;8:1303-1308.

36. Zhang QJ, McMillin SL, Tanner JM, Palionyte M, Abel ED, Symons JD. Endothelial nitric oxide synthase phosphorylation in treadmill-running mice: role of vascular signalling kinases. J Physiol.London 2009;587:3911-3920.

37. Chien S. Mechanotransduction and endothelial cell homeostasis: the wisdom of the cell. Am J Physiol-Heart Circul Physiol. 2007;292:H1209-H1224.

38. Jaalouk DE, Lammerding J. Mechanotransduction gone awry. Nat Rev Mol Cell Biol. 2009;10:63-73.

39. dela Paz N, Melchior B, Frangos J. Shear stress induces G protein-coupled receptor (GPCR)-independent heterotrimeric G protein activation in endothelial cells. FASEB J. 2015;29:1.

40. Ramage L, Nuki G, Salter DM. Signalling cascades in mechanotransduction: cell-matrix interactions and mechanical loading. Scand J Med Sci Sports 2009;19:457-469.

41. Eter N, Gobbels M. A new technique for tear film fluorophotometry. Br J Ophthalmol. 2002;86:616-619.

42. Shi B, Han B, Schwab IR, Isseroff RR. UVB irradiation-induced changes in the 27-kd heat shock protein (HSP27) in human corneal epithelial cells. Cornea 2006;25:948-955.

43. Jauhonen HM, Kauppinen A, Paimela T, Laihia JK, Leino L, Salminen A, et al. Cis-urocanic acid inhibits SAPK/JNK signaling pathway in UV-B exposed human corneal epithelial cells in vitro. Mol Vis. 2011;17:2311-2317.

44. Lu L, Wang L, Shell B. UV-induced signaling pathways associated with corneal epithelial cell apoptosis. Invest Ophthalmol Vis Sci. 2003;44:5102-5109.

45. Kim JY, Kang SS, Kim ES, Kim MJ, Tchah H. Epithelial wound healing and heat shock protein 27 phosphorylation in NaCl-induced hyperosmolar condition. Invest Ophthalmol Vis Sci. 2015;56:2.

46. Chen M, Hu DN, Pan Z, Lu CW, Xue CY, Aass I. Curcumin protects against hyperosmoticity-induced IL-1 beta elevation in human corneal epithelial cell via MAPK pathways. Exp Eye Res. 2010;90:437-443.

47. Corrales RM, Luo LH, Chang EY, Pflugfelder SC. Effects of osmoprotectants on hyperosmolar stress in cultured human corneal epithelial cells. Cornea 2008;27:574-579.

48. Wang L, Dai W, Lu L. hyperosmotic stress-induced corneal epithelial cell death through activation of polo-like kinase 3 and c-Jun. Invest Ophthalmol Vis Sci. 2011;52:3200-3206.

49. Shi L, Yu XM, Yang HL, Wu XY. Advanced glycation end products induce human corneal epithelial cells apoptosis through generation of reactive oxygen species and activation of JNK and p38 MAPK pathways. PLoS One 2013;8:e66781.

50. Song IS, Kang SS, Kim ES, Park HM, Choi CY, Tchah H, et al. Heat shock protein 27 phosphorylation is involved in epithelial cell apoptosis as well as epithelial migration during corneal epithelial wound healing. Exp Eye Res. 2014;118:36-41.

51. Mengistu M, Brotzman H, Ghadiali S, Lowe-Krentz L. Fluid shear stress-induced JNK activity leads to actin remodeling for cell alignment. J Cell Physiol. 2011;226:110-121.

52. Okada Y, Saika S, Shirai K, et al. JNK MAPK signaling contributes in vivo to injury-induced corneal epithelial migration. Ophthalmic Res. 2009;42:185-192.

53. Kimura K, Teranishi S, Yamauchi J, Nishida T. Role of JNK-dependent serine phosphorylation of paxillin in migration of corneal epithelial cells during wound closure. Invest Ophthalmol Vis Sci. 2008;49:125-132.

54. Ogawa H, Kozhemyakina E, Hung HH, Grodzinsky AJ, Lassar AB. Mechanical motion promotes expression of Prg4 in articular cartilage via multiple CREB-dependent, fluid flow shear stress-induced signaling pathways. Genes Dev. 2014;28:127-139.

55. Kido S, Kuriwaka-Kido R, Imamura T, Ito Y, Inoue D, Matsumoto T. Mechanical stress induces Interleukin-11 expression to stimulate osteoblast differentiation. Bone 2009;45:1125-1132.

56. Ogasawara A, Arakawa T, Kaneda T, Takuma T, Sato T, Kaneko H, et al. Fluid shear stress-induced cyclooxygenase-2 expression is mediated by C/EBP beta, cAMP-response element-binding protein, and AP-1 in osteoblastic MC3T3-E1 cells. J Biol Chem. 2001;276:7048-7054.

57. Alenghat FJ, Tytell JD, Thodeti CK, Derrien A, Ingber DF. Mechanical control of cAMP signaling through integrins is mediated by the heterotrimeric Galphas protein. J Cell Biochem. 2009;106:529-538.

58. Meyer CJ, Alenghat FJ, Rim P, Fong JH, Fabry B, Ingber DE. Mechanical control of cyclic AMP signalling and gene transcription through integrins. Nat Cell Biol. 2000;2:666-668.

59. Sterner O, Karageorgaki C, Zurcher M, et al. Reducing friction in the eye: a comparative study of lubrication by surface-anchored synthetic and natural ocular mucin analogues. ACS Appl Mater Interfaces 2017;9:20150-20160.

Supporting information

Development of an in vitro model to study the biological effect of blinking

Guoting Qin[1], Hasna Baidouri[1], Adrian Glasser[1], VijayKrishna Raghunathan[1], Carol Morris[2], Inna Maltseva[2], Alison M. McDermott[1]

1. Data Analysis of the Human Phospho-kinase Array Assay

Each array has capture and control antibodies spotted on the nitrocellulose membrane. After incubation with lysates of control cells (Ctrl), and cells subjected to sweep cycles of 0 mN (0 mN) and 19.6 mN (19.6 mN), the membranes were processed per the manufacturer's instruction. The x-ray film was scanned and saved as a Tiff image file (Figure S1). The intensity of each spot was determined using a Matlab program, and was correlated with each protein target according to the coordinates provided by the manufacturer (Table S1).

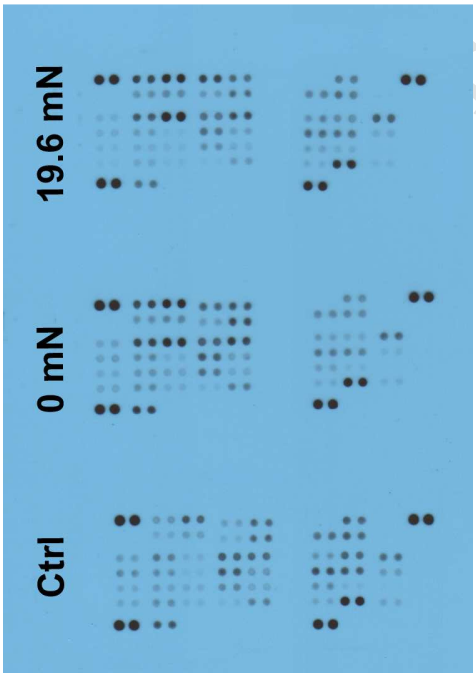

Figure S1. A typical x-ray film image showing human phospho-kinase arrays of various samples.

Table S1. Human phospho-Kinase array coordinates provided by the manufacturer.

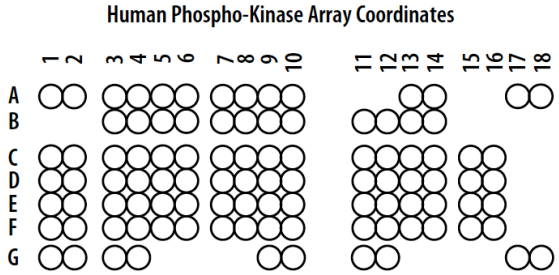

Membrane/ Coordinate	Target/Control	Membrane/ Coordinate	Target/Control
A-A1, A2	Reference Spot	A-F3, F4	Chk-2
A-A3, A4	p38α	A-F5, F6	FAK
A-A5, A6	ERK1/2	A-F7, F8	PDGF Rβ
A-A7, A8	JNK 1/2/3	A-F9, F10	STAT5a/b
A-A9, A10	GSK-3α/β	A-G1, G2	Reference Spot
A-B3, B4	EGF R	A-G3, G4	PRAS40
A-B5, B6	MSK1/2	A-G9, G10	PBS (Negative Control)
A-B7, B8	AMPKα1	B-A13, A14	p53
A-B9, B10	Akt 1/2/3	B-A17, A18	Reference Spot
A-C1, C2	TOR	B-B11, B12	Akt 1/2/3
A-C3, C4	CREB	B-B13, B14	p53

A-C5, C6	HSP27	B-C11, C12	p70 S6 Kinase
A-C7, C8	AMPKα2	B-C13, C14	p53
A-C9, C10	β-Catenin	B-C15, C16	c-Jun
A-D1, D2	Src	B-D11, D12	p70 S6 Kinase
A-D3, D4	Lyn	B-D13, D14	RSK1/2/3
A-D5, D6	Lck	B-D15, D16	eNOS
A-D7, D8	STAT2	B-E11, E12	STAT3
A-D9, D10	STAT5a	B-E13, E14	p27
A-E1, E2	Fyn	B-E15, E16	PLC-γ1
A-E3, E4	Yes	B-F11, F12	STAT3
A-E5, E6	Fgr	B-F13, F14	WNK1
A-E7, E8	STAT6	B-F15, F16	PYK2
A-E9, E10	STAT5b	B-G11, G12	HSP60
A-F1, F2	Hck	B-G17, G18	PBS (Negative Control)

2. Summary of Human Phospho-kinase Array Assay Results from three Independent Experiments.

Table S2. Summary of the relative changes of phosphorylation levels of 43 kinase phosphorylation sites and 2 related proteins (β-catenin and HSP60) of hTCEpi cells subjected to sweep cycles with force (19.6 mN) compared to control samples. Orange, white and green boxes represent increased, stable, and decreased levels of phosphorylation of protein kinases or amount of total protein (β-catenin and HSP60) in treated samples compared to control samples from three independent experiments. Purple highlights the four protein kinases whose phosphorylation

levels were quantitated using ELISA. These were selected as three (p38α, JNK1/2/3 and HSP27) were consistently increased in all three experiments and one (CREB) showed variable changes in each experiment.

	Exp 1	Exp 2	Exp 3
p38α			
ERK1/2			
JNK 1/2/3			
GSK-3α/β			
EGF R			
MSK1/2			
AMPKα1			
Akt 1/2/3 (S473)			
TOR			
CREB			
HSP27			
AMPKα2			
β-Catenin			
Src			
Lyn			
Lck			
STAT2			
STAT5a			
Fyn			
Yes			
Fgr			
STAT6			
STAT5b			
Hck			
Chk-2			
FAK			
PDGF Rβ			
STAT5a/b			
PRAS40			
p53 (S392)			
Akt 1/2/3 (T308)			
p53 (S46)			
p70 S6 Kinase (T389)			
p53 (S15)			
c-Jun			
p70 S6 Kinase (T421/S424)			
RSK1/2/3			
eNOS			
STAT3 (Y705)			
p27			
PLC-γ1			
STAT3 (S727)			
WNK1			
PYK2			
HSP60			

Phosphorylation levels of protein kinases or amount of total protein (β-catenin & HSP60):
19.6 mN vs. Ctrl

decreased
stable
increased

protein kinase quantitated using ELISA

3. Estimation of shear stress experienced by cells undergoing sweeping cycles without force.

We first determined the viscosity of the growth medium (0.83 mPa.s, experimentally determined) at 37 °C using water at 22 °C (1.06 mPa.s, experimentally determined) and 37 °C (0.69 mPa.s, Perry's handbook) as standards using a Thermo Scientific Haake Mars 60 Rheometer. Growth medium exhibited Newtonian behavior under the conditions tested. We then assumed that the arm traverses parallel to the cellular surface.

Using equations for parallel plate shear, $\tau = \mu_{media} * \frac{\partial U}{\partial h}$

where, τ = shear stress, μ_{media} = viscosity of media, U = shear rate, and h = height of the media, we determined the shear stress applied by the arm in the absence of a downward load to be in the range of 0.57 – 1.10 dyne/cm^2.

4. Cell Layer Thickness for Cells on Membrane Inserts Treated with Higher Forces (98.1 mN and 196.1 mN).

A significant decrease in cell layer thickness was found for cells treated with forces of 98.1 mN and 196.1 mN for 1 h and 3 h, respectively. These data showed that some cells were swept off from the membrane under large mechanical forces, indicating severe gross damage.

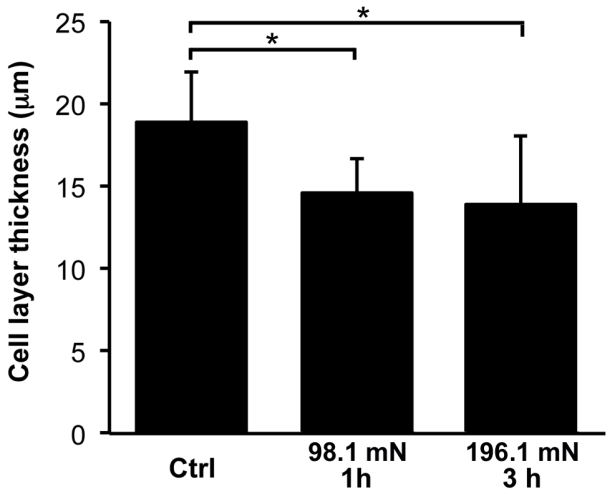

Figure S2. Cell layer thicknesses of samples without treatment (Ctrl) and treated with 98.1 mN g for 1 h or 196.1 mN for 3 h. Data are expressed as mean ± SD from 27-33 measurements. Statistical analysis was performed using one-way ANOVA followed by Tukey's test where significance was found. * $P<0.05$.